JOURNAL OF APPLIED SCIENCE AND TECHNOLOGY TRENDS

Attitude Mounting Misalignment Estimation Method for the Calibration of UAV LiDAR System by using a TIN-based Corresponding Model

Daniel Rodrigues dos Santos[1,*], Leonardo Ercolin Filho[1], Paulo Sérgio de Oliveira Jr.[1], Henrique Cândido de Oliveira[2]

[1]*Federal University of Parana, Department of Geomatics, Brazil, danielsantos@ufpr.br, leonardo.ercolin@ufpr.br, paulo.junior@ufpr.br*
[2]*State University of Campinas, Faculty of Civil Engineering, Architecture and Urbanism, Brazil, oliveira@fec.unicamp.br*
Correspondence: danielsantos@ufpr.br

Abstract

In traditional attitude mounting misalignment estimation methods for the calibration of unmanned autonomous vehicle (UAV) based light detection and ranging (LiDAR) system, signalized targets and iterative corresponding models are required, which makes it highly cost and computationally time-consuming. This paper presents an attitude mounting misalignment estimation (AMME) method for the calibration of UAV LiDAR system. The proposed method is divided into the coarse registration of LiDAR strips and the estimation of the attitude mounting misalignment. Firstly, 3D keypoints are extracted in the point clouds using the scale-invariant feature transform (SIFT) algorithm. Afterwards, the point feature transform (PFH) descriptor is used for 3D keypoint matching. Then, the coarse registration is executed. In the second part of the contribution, the systematic errors in the attitude mounting misalignment are estimated by incorporating the proposed triangular irregular network (TIN) corresponding model into the calibration modelling. Using the TIN-based corresponding model saves time and cost for AMME method. Furthermore, it provides two important effects: practical and computational, as no designed calibration boards, segmentation and iterative matching are needed. The performance of the proposed method is demonstrated under an UAV LiDAR data onboarded with lightweight navigation sensors. The experimental results show the efficacy of the method in comparison with a state-of-the-art method.

Keywords: UAV LiDAR system, calibration, attitude mounting misalignment, TIN-based corresponding model

Received: August 6th, 2020/ Accepted: December 16th, 2020/Online: December 28th, 2020

I. INTRODUCTION

A goal in geomatics is to develop a mobile mapping system that can capture georeferenced 3D point clouds with positional accuracy. Within various ascendant geo-technologies for spatial data acquisition, unmanned autonomous vehicle (UAV) based light detection and ranging (LiDAR) systems are highly attractive because of their lightweight and ability to derive point clouds with very high and homogeneous point density from the environment.

During the mapping process, laser unit measurements, the estimated platform's trajectory obtained from a Global Navigation Satellite System (GNSS) and an inertial navigation system (INS) should be properly integrated with demanding accuracy. In addition, the mounting parameters between LiDAR and the integrated GNSS/INS sensors must be achieved to allow UAV LiDAR systems to derive 3D point clouds with centimetric positional accuracy. However, due to the systematic errors of a UAV LiDAR data derived from GNSS/INS errors and boresight angular error, point clouds derived with high positional accuracy face a challenge. They must efficiently detect the systematic georeferencing errors re-estimating the entire UAV LiDAR system mounting parameters. This procedure is known as attitude mounting misalignment calibration (AMMC).

Although existing AMMC methods are functional, they require manual procedure for signalized targets, primitive-based or ground-based

approaches, and high computational cost. This paper presents a triangular irregular network (TIN)-based corresponding model for estimating attitude mounting misalignment to derive a high positional 3D point cloud. A keypoint-based approach to avoid iterative matching is also used. The proposed method demonstrates that the introduction of a TIN-based corresponding model can promote the practical effect at the AMMC and at computational cost while segmentation and iterative matching are not needed. The experiments show the role of AMMC in the accuracy of the 3D point clouds. It also demonstrates that the TIN-based corresponding model can estimate attitude mounting misalignment without iterative matching.

This paper is organized as follows. Section II reviews the related works in AMMC. In Section III, the TIN-based corresponding model is given in detail. Section IV describes the experiments and results obtained using the proposed method. Finally, the paper is concluded in Section V.

II. RELATED WORKS

During the last decade, the AMMC problem has been intensively researched. These approaches are assembled into two different groups: (1) strip adjustment and (2) AMMC methods. In strip adjustment methods, the systematic errors are modelled in the object domain. Surfaces or features derived from the LiDAR data natural are widely used to find the transformation parameters between overlapping LiDAR strips. In Kilian et al. [1], a polynomial model was previously introduced to determine the discrepancy over LiDAR strips. Although it allows the tridimensional assessment of relative accuracy, designed calibration boards covered by highly reflective surfaces are mandatory. To avoid calibration field boards, a plane-based approach is proposed in [2]. The LiDAR data accuracy is achieved via surfaces previously matched. Vosselman [3] formerly introduced linear features for the strip adjustment procedure. In Van der Sande et al. [4], point-to-plane distances were reliably used as observables into least-squares method (LSM) for the assessment of relative accuracy of LiDAR data. According to Filin [5], non-rigorous approaches focus on the effect of the systematic errors omitting the causes of the source errors derived from lightweight GNSS/INS and laser sensors onboard the UAV. Furthermore, primitives rely on segmentation, in which there are computationally non-attractive, manual interventions might be necessary and can affect the quality of the adjustment step.

By contrast to strip adjustment approaches, AMMC methods investigate the sources derived from systematic errors. Furthermore, the attitude mounting misalignment and other calibration parameters can be used to model the point cloud. In Skaloud and Lichti [6], gabled roofs were manually extracted in the LiDAR data, and a constraint is used to assurance reliability in the LSM mounting parameters solution. Although, no additional calibration field is needing the method depends on segmentation procedures. In Habib et al. [7], the effect of the systematic errors was modelled calculating the discrepancies between pairs of LiDAR strips, while the trajectory errors were used for the estimation of the mounting parameters. The authors proposed a variant of iterative closest point, proposed by [8], to find the patch correspondences, called ICPatch. However, the

mentioned algorithm is iterative and time consuming. A spline trajectory correction model for the modelling of trajectory errors was previously proposed in [9]. A point-to-plane corresponding model was previously used to the estimation of the mounting parameters jointly with the correction errors task. This is done iteratively using the residual vector between closest points and their normal vectors. In Ravi et al. [10], primitive-based were used to find the attitude mounting misalignment of a UAV LiDAR system onboarded with lightweight positional, inertial and active sensors. However, the authors used a designed calibration board for the automatic identification of primitive correspondences. Furthermore, the method also depends on rigorous flight configurations. A variant of the [9] also was used for AMMC of a mobile terrestrial and UAV LiDAR systems in [11]. However, the method is computationally non-attractive and manual interventions are mandatory. Zhang et al. [12] have presented a mounting parameters error rectification approach, which aims at the iterative updating of boresight errors using 3D matched points obtained on laser intensity information. For each iteration an approximate solution is obtained using the LSM. Although efficient, the algorithm is highly time-consuming. In de Oliveira and dos Santos [13], a AMMC of UAV LiDAR systems with refinement of the attitude mounting misalignment using a point-to-plane approach was previously presented. The mounting parameters are estimated conditioning the centroid of a plane segmented to lie on its corresponding segmented plane without an additional surveying campaign. Then, the attitude mounting misalignment are refined using a new point-to-plane model. Although the proposed constraint can guarantee that the calibration parameters are correctly estimated even when the GNSS/INS trajectory is highly noised, is highly demanded the iterative refinement of the attitude mounting misalignment. It also depends on segmentation.
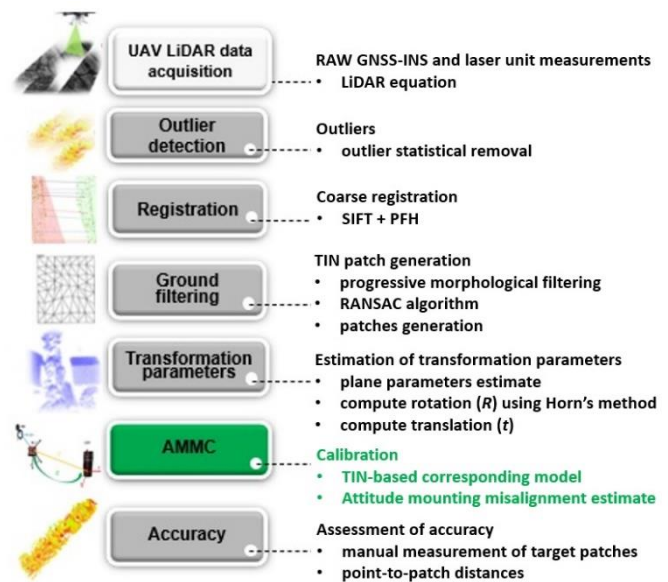

Fig. 1. Generic structure of the proposed method.

Contrary to the aforementioned approaches, using the TIN-based corresponding proposed model saves time and computational cost for AMMC, as no designed calibration

boards and segmentation are needed. It can also avoid iterative matching, as used for the ICPatch algorithm.

III. ATTITUDE MOUNTING MISALIGNMENT

This paper follows the concept of AMMC by using a TIN-based corresponding model. The main aspect of this approach is the development of a TIN-based corresponding model for AMMC. The architecture of the proposed AMMC method consists of six main steps, as illustrated in Figure 1. In particular, it uses a non-iterative TIN-based approach without segmentation requirements.

From the raw UAV LiDAR data, a set of 3D point clouds are created. Secondly, the proposed method uses a statistical outlier removal algorithm in order to detect and remove outliers [14]. Afterwards, a keypoint-based coarse registration by combining an adaptation of scale invariant feature transform (SIFT) algorithm with the formulation of the point feature histogram (PFH) descriptor [15] is used to coarse registration step. Fourthly, gabled roofs are extracted by combining the progressive morphological filter [16] and the random sample consensus algorithm [17]. Thus, the transformation parameters jointly with the plane parameters are estimated. Finally, a TIN-based corresponding model is incorporated into the functional model of the AMMC method for the estimation of the attitude mounting misalignment.

A. Point cloud generation by using the LiDAR Equation

Typically, three coordinate systems, namely, mapping frame (m), INS body frame (b) and laser unit frame (l) are involved in the LiDAR Equation. The $p_j^m(t)$ in the time ti can be written as:

$$p_j^m(ti) = a_{nav}^m(ti) + r_b^m(ti)\left[r_l^b r_j^l(ti) + a_{nav}^b\right] \quad (1)$$

where $a_{nav}^m(ti)$ represents the position at time ti of the GNSS/INS in m, $r_b^m(ti)$ is the attitude between the INS and m, r_l^b denotes the boresight matrix between the laser unit and the INS, $r_j^l(ti)$ is the coordinate vector of *j-th* point in l and a_{nav}^b the fixed lever-arm vector.

B. Outlier detection and filtering

In point cloud processing, noise points can easily corrupt matching process. Thus, detect and remove outliers is an important step for future procedures. Herein, the outliers are detected by analysing a query point p_q with respect to its surrounding neighbours k via the statistical outlier removal algorithm [14]. Basically, given a reference strip ($\aleph$), the mean distance d_p between each $p_q \in \aleph$ and its k neighbours is computed, resulting in a filtered strip ($\aleph'$).

C. Coarse registration by keypoint-based approach

The keypoint-based coarse registration is used by combining an adaptation of SIFT algorithm with the PFH's descriptor formulation [15]. Firstly, the SIFT algorithm detect edges in 3D using difference-of-gaussian scale-space. Afterwards, a search radius is selected and the normal of each point into search radius is computed. Then, a Darboux frame with origin at 3D keypoint is computed for each pair of points, as follows:

$$\begin{cases} e = n \\ u = e \times \dfrac{(p_i - p_j)}{\|p_i - p_j\|} \\ v = e \times u \end{cases} \quad (2)$$

where n represents the normal vector of point.

Thus, the actual descriptors for (p_i, p_j) can be computed to express the difference between n and those of its neighbourhood points p_j [15]:

$$\begin{cases} \alpha = arccos(u \cdot n) \\ \beta = arccos\left(e \cdot \dfrac{(p_i - p_j)}{\|p_i - p_j\|}\right) \\ \Omega = arctan(v \cdot n, e \cdot n) \\ d = \|p_i - p_j\| \end{cases} \quad (3)$$

where d represents the distance between the origins of the coordinate systems.

The PFH algorithm generate a 33-bin PFH histogram for each pair of LiDAR strip. Thus, the correspondences are established, and the initial transformation parameters are coarsely estimated a transformation using a global affine transformation matrix, as follows:

$$p_i = Fp_j + b \quad (4)$$

where p_i and p_j are pairs of corresponding 3D key points, F represents a coefficient matrix, and b is the translation vector.

D. Estimation of the attitude mounting misalignment by using the proposed TIN-based corresponding model

This paper introduces a TIN-based corresponding model to estimate the attitude mounting misalignment minimizing the sum of the distance between points and corresponding TIN patches. Typically, the TIN structure is formed with several planar patches. Thus, to reduce the number of existing primitives in the LiDAR strips, a progressive morphological filter [16] is used. Firstly, an erosion followed by a dilation process is applied. The large non-ground objects remain while small vegetation is removed. Secondly, the height difference between the original LiDAR data and the initial filtered surface is calculated. Again, the erosion followed by dilation is executed. Finally, a new filtered surface is determined. The gabled roof is remained in the point cloud, while the vegetation is removed using the random sample consensus algorithm [17].

Herein, a TIN is created from gabled roof objects using the method described in [18]. This paper recovers the TIN patch parameters jointly with the transformation parameters in a combined LSM solution expressed as:

$$\langle n_T, c, R, t \rangle \quad (5)$$

where $n_T = \left[n_x, n_y, n_z\right]^T$, R is the 3x3 rotation parameters and t is the 3x1 translation parameter. The method uses the constrain introduced in [13] to forces the centroids (c) to belong to its corresponding patch.

Thus, each point p_T in the target point cloud $\aleph'$ is computed via the intersection between an orthogonal projected line from p_R to its corresponding TIN patch into the reference point cloud $\beth'$ (see Figure 2).
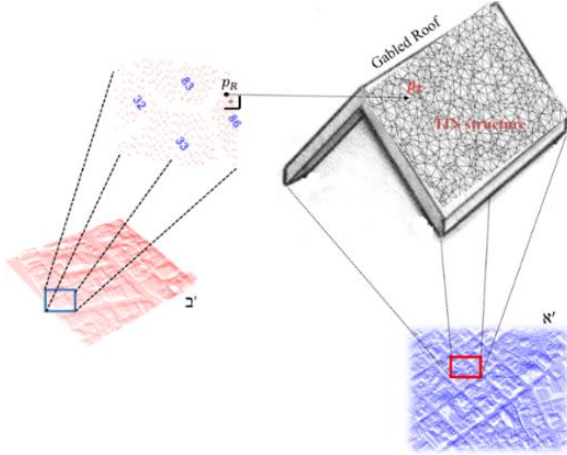

Fig. 2. Conceptual basis of the proposed corresponding model.

The intersection between a orthogonal projected line and a TIN patch is as follows:

$$p_T = p_R + s n_T \tag{6}$$

where $n_T = (n_x, n_y, n_z)^T$, $s = d_T - n_T p_R'$, d_T represent the perpendicular distance from the origin to n_T and $p_R' = R p_R + t$ that represents the transformation from p_R to p_T consists of a 3D rigid motion.

Thus, Equation (6) can be rewritten as follows:

$$p_T = p_R + [d_T - n_T(R p_R + t)] n_T \tag{7}$$

From Equation (7) can be express the following sentence:

$$p_T - p_R = 0 = [d_T - n_T(R p_R + t)] n_T \tag{8}$$

$$n_T d_T - n_T(n_T R p_R) + n_T(n_T t) = 0 \tag{9}$$

$$n_T(d_T - d_T') + n_T(n_T t) = 0 \tag{10}$$

$$n_T t = d_T - d_T' \tag{11}$$

The rotation R can be estimated as follows:

$$n_T' = R n_T \tag{12}$$

Assuming that for each pair of LiDAR strip exists a rotational and translational $(R_{\beth i}, t_{\aleph j})$ parameters, for $i = 0, \ldots, k$

and $j = i + 1$; by substituting Equation (1) in the p_R of Equation (7) and rearranging the terms of this equation, the following expression is obtained:

$$n_T T = -d_T \tag{13}$$

where $T = R_{\beth i} \left(n_T{}^T \left[a_{nav}^m(t) + r_b^m(t) [r_l^b r_j^l + a_{nav}^b] \right] \right) + t_{\aleph j}$.

Thus, three separate sets of equations per TIN correspondences are formulated, one for estimation of $t_{\aleph j}$ (see eq. 11), in which the LSM solution can be solved by using equations $Bt = y + e$, where B and y are obtained by assembling n_T and $d_T - d_T'$ for all TIN-to-TIN correspondences and e contains the residual values.

The LSM solution for $t_{\aleph j}$ can be obtained as: $\widehat{t_{\aleph J}} = (B^T B)^{-1} B^T y$. The second equation for the estimation of $R_{\beth i}$ (see eq. 12), in which is obtained using Horn's solution [19]. The third equation for the estimation of the attitude mounting misalignment $r_l^b(\Delta \kappa, \Delta \varphi, \Delta \omega)$, as observed in Equation (13). The LSM solution for r_l^b can be obtained as: $Jx = y + e$. The goal of the LSM is to minimise the sum of all squared point-to-TIN patches.

In the subsequent section, we describe the experiments. Note that, admitting a rough coarse registration estimate $p_T - p_R = 0$, as presented in Equation (8). Thus, both transformation parameters and attitude mounting misalignment are estimated without iterative matching.

IV. EXPERIMENTS AND ANALYSIS

To demonstrate the effectiveness of the proposed AMMC method, six flight trajectories were previously captured with the Velodyne VLP-16 Puck HI-RES laser scanner integrated with an Applanix APX-15 onboard on a DJI S1000 UAV platform. The accuracy achieved after post-processing with the POSPac software from Applanix is 0.025^0 for pitch/roll and 0.08^0 for yaw, and the position accuracy is 0.02–0.05 m [13]. For the experiments, two flight lines with a 100% overlap in opposite directions and a flying height of 30 m, two flight lines with a 50% in the same direction overlap and a flying height of 60 m, one flight line with a 30% overlap with respect to flight line 1 and the same direction, and one flight line with 30% overlap with respect to flight line 3.

The point clouds for each flight line were derived by using initial values of the attitude mounting misalignment set as a vector of zeros at the LiDAR equation. The positional offset between LiDAR relating to the GNSS/INS sensor were previously determined to better than 0.2 cm by topographic survey. Thus, the filtering process steps were previously executed. Afterwards, TIN structures were created from gabled roofs. The TIN patches extracted using the described tasks performed in light of the proposed method, is depicted in Fig 3.
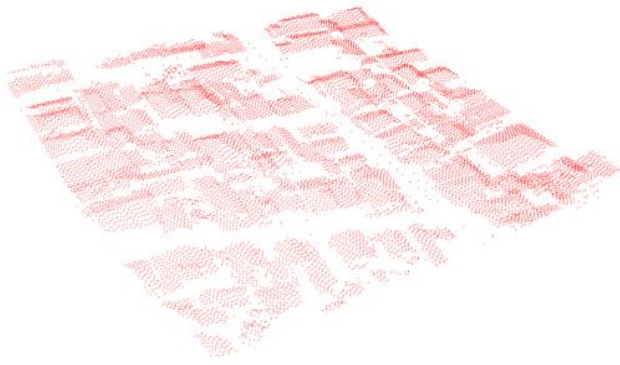
Fig. 3. TIN patches generated through proposed pre-processing steps.

Thus, the transformation parameters and the plane parameters are simultaneously estimated. Then, the attitude mounting misalignment are estimated based on the proposed TIN corresponding model.
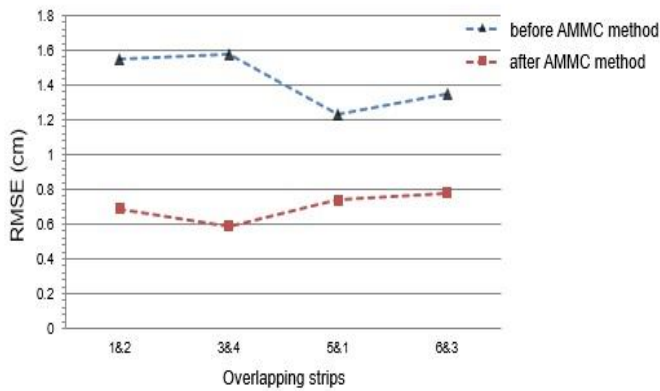

Fig. 4. RMSE of the point-to-TIN patch distances before and after AMMC method for each overlapping strip.

The point-to-TIN patch distances between the manually extracted check-targets in the reference point cloud and the transformed point coordinates obtained after the attitude mounting misalignment calibration provide an indication of the discrepancies between the overlapping strips. Figure 4 shows the root square mean error (RMSE) of the point-to-TIN patch distances before and after AMMC method for each overlapping strip.

Table I. Estimated attitude mounting misalignment using the TIN-based corresponding model.

Attitude mounting misalignment		
$\Delta\kappa$ (degree)	$\Delta\varphi$ (degree)	$\Delta\omega$ (degree)
0.014±0.021	-0.0122±0.0017	0.001±0.0154

Table I lists the attitude mounting misalignment estimated using the proposed method. The original LiDAR strips were reconstructed using the set of estimated attitudes. Fig. 5 shows a portion of the generated point cloud before and after AMMC method.
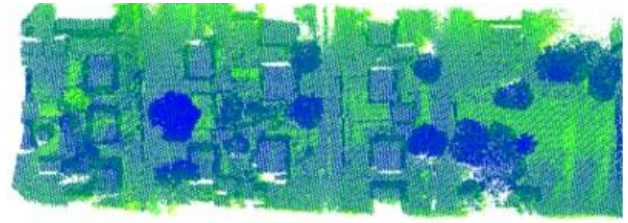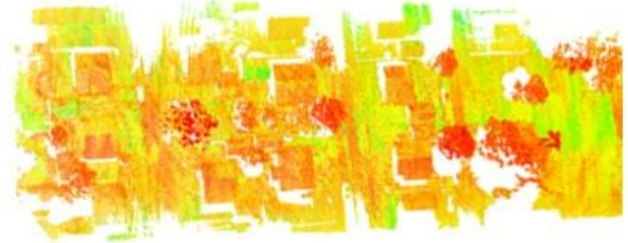
Fig. 5. Generated 3D point cloud before (a) and after (b) proposed AMMC method.

An example of a 3D point cloud of an urban environment, with different point of views, obtained with the proposed method is shown in Fig. 6.
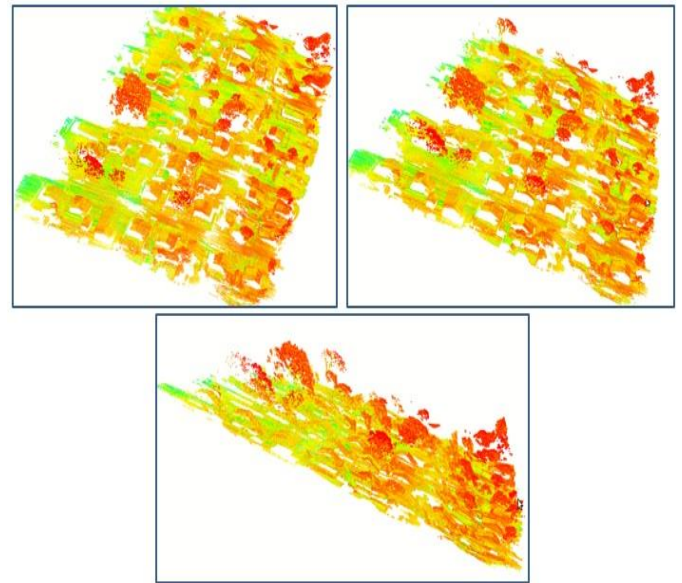

Fig. 6. 3D point cloud derived from the proposed method.

For the quantitative assessment of the derived 3D point cloud from the proposed method, well-distributed target check points associated with their corresponding patches in the derived point cloud (see Fig. 7) were surveyed with a GNSS sensor. The mean and standard deviation of the point-to-TIN patch distances were computed. After the AMMC, the mean range from -1.5 cm to 1.2 cm, whereas the standard deviations range from 1.1 cm to 1.5 cm. Evidently, the proposed TIN-based corresponding model enables refined attitude mounting misalignment values. The mean computing time was around 100 s.
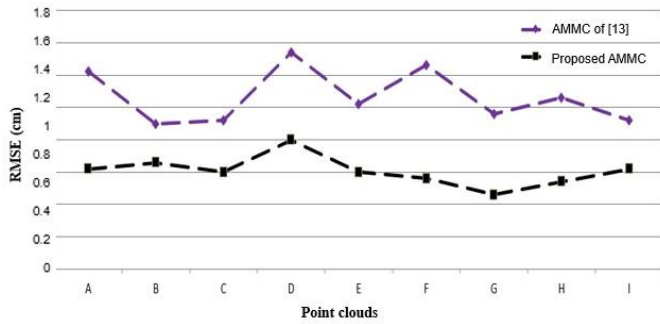
Fig. 7. RMSE of the point-to-TIN patch distances before and after proposed AMMC and the method of [13].

As a sanity check, the proposed method has been compared with the method of [13]. The RMSE of the normal distance of points from their corresponding planar patches was calculated for results obtained with the proposed AMMC method and the method of [13]. Fig. 6 shows the RMSE values obtained with the proposed method and the RMSE values obtained with the method of [13].

A. Discussions

The proposed method was implemented with C++ by using Point Cloud Library on an Intel 3.60 GHz i7 CPU, 8 GB memory Ubuntu system. The testing procedure is performed offline and includes the following: (1) extraction of SIFT features, (2) matching of keypoints, (3) estimation of the initial transformation, (4) ground filtering process, (5) normal planar patch estimation jointly with the estimation of the transformation parameters, and (6) AMMC method. The estimation of the initial transformation with 3D keypoints generated via [15] is fast and essential to achieve good initial transformation for the attitude mounting misalignment. The main novelty of this work is the proposed TIN-based corresponding model without iterative matching procedure. It can incorporate a large number of reliable corresponding point-to-TIN patches, increasing its performance. The worst $\Delta\kappa$ estimation is most likely caused by the weak geometry of the patches. The attitude misalignments $\Delta\varphi$ and $\Delta\omega$ are less sensitive and, consequently, are more precisely estimated. Good geometry thanks to significant variations in gabled roofs. Compared with plane-based approaches, the proposed method does not require planar segmentation. The method proposed in this study has the following advantages: (1) it is robust for outliers, (2) it is independent of the data mass, (3) it has better accuracy and saves more computational cost than [13], and (4) it exploits the full geometric richness of the scene by combining points and patches for the estimation of the attitude mounting misalignment. The main limitations are as follows: (1) the proposed model can only be used in environments modified by humans and (2) the lack of planar patches with different configurations affects the performance of the method, causing inconsistency in the refinement procedure. Notably, UAV LiDAR systems are being increasingly used in many geoscience applications, such as mapping, forestry inventory, power line inspection, vegetation management, hydrologic modelling and urban design.

V. CONCLUSIONS AND FUTURE WORKS

This paper presents an effective implementation for attitude mounting misalignment estimation method for the calibration of UAV LiDAR system. The proposed TIN-based corresponding model is quite robust for the estimation of the attitude mounting misalignment. This work exploits both points and patches within the calibration method. Firstly, the keypoint-based coarse registration step is used to estimate an initial transformation between LiDAR strips. Secondly, TIN patches are employed. The consequence is the important computational effect of having no both planar segmentation procedure and iterative matching requirements. The effectiveness of the proposed TIN-based corresponding model has been verified and can also be applied to other model fitting problems. The introduction of the proposed TIN-based corresponding model can estimate attitude mounting misalignment parameters without an iterative matching procedure. In the future, the proposed corresponding model will be improved for the use of multi-features and will be deployed on a mobile terrestrial platform.

REFERENCES

[1] J. Kilian, N. Haala, M. Englich, "Capture and evaluation of airborne laser scanner data", In Proceedings of International Archives of the Photogram., Remote Sens. and Spatial Inform. Sciences, Vienna, Austria, 12-18 July 1996, pp. 383-388.

[2] D. Latypov, "Estimating relative LiDAR accuracy information from overlapping flight lines", ISPRS J. Photogramm. Remote Sens., vol. 56, pp. 236-245, 2002.

[3] G. Vosselman, "Strip offset estimation using linear features", In Proceedings of the 3rd International Workshop on Mapping Geo-Surfical Processes Using Laser Altimetry, Columbus, OH, USA, 2002, pp. 1-9.

[4] C. Van der Sande, S. Soudarissanane, K. Khoshelham, "Assessment of relative accuracy of AHN-2 laser scanning data using planar features", Sensors, vol. 10, pp. 8198–8214, 2010.

[5] S. Filin, "Recovery of systematic biases in laser altimetry data using natural surfaces", Photogramm. Eng. and Remote Sens. Vol. 69, pp. 1235-1242, 2003.

[6] J. Skaloud, D. Lichti, "Rigorous approach to bore-sight self-calibration in airborne laser scanning", ISPRS J. Photogram. Remote Sens. Vol. 61, pp. 47–59, 2006.

[7] A. Habib, A.P. Kersting, K.I. Bang, D.C. Lee, "Alternative Methodologies for the Internal Quality Control of Parallel LiDAR Strips", IEEE Trans. Geosci. Remote Sens., vol. 48, pp. 221-236, 2010.

[8] P. Besl, N.D. Mckay, "A method for registration of 3-D shapes", IEEE Trans. Pattern Anal., Mach. Intell., vol. 14, pp. 239-256, 1992.

[9] P. Glira, N. Pfeifer, G. Mandlburger, "Rigorous strip adjustment of UAV-based laserscanning data including time-dependent correction of trajectory errors", Photogramm. Eng. Remote Sens. vol. 82, pp. 945-954, 2016.

[10] R. Ravi, T. Shamseldin, M. Elbahnasawy, Y.J. Lin, A. Habib, " Bias Impact Analysis and Calibration of UAV-Based Mobile LiDAR System with Spinning Multi-Beam Laser Scanner", Applied Sciences. Vol. 8, pp. 297, 2018.

[11] Z. Li, J. Tan, H. Liu, "Rigorous Boresight Self-Calibration of Mobile and UAV LiDAR Scanning Systems by Strip Adjustment", Remote Sens., vol. 11, pp. 420-442, 2019.

[12] X. Zhang, R. Gao, Q. Sun, J. Cheng, "An automated rectification method for unmanned aerial vehicle lidar point cloud data based on laser intensity", Remote Sens., vol. 11, pp. 811–830, 2019.

[13] E.M. de Oliveira Jr, D.R. dos Santos, "Rigorous Calibration of UAV-Based LiDAR Systems with Refinement of the Boresight Angles Using a Point-to-Plane Approach", Sensors, vol. 19, p. 5224, 2019.

[14] R.B. Rusu, N. Blodow, Z. Marton, A. Soos, M. Beetz, "Towards 3D object maps for autonomous household robots" In International Conference on Intelligent Robots and Systems, IEEE. https://doi.org/10.1109/iros.2007.4399309, 2007.

[15] R.B. Rusu, N. Blodow, M. Beetz, "Fast point feature histograms (FPFH) for 3D registration", IEEE International Conference on obotics and Automation (ICRA), pp. 3212-3217, 2009.

[16] K. Zhang, S. Chen, D. Whitman, M. Shyu, J., Yan, C. Zhang, "A progressive morphological filter for removing nonground measurements from airborne LiDAR data" IEEE Transactions on Geoscience and Remote Sensing, vol. 41, pp. 872-882, 2003.

[17] M.A. Fischler, R.C. Bolles, "Random sample consensus: A paradigm for model fitting with applications to image analysis and automated cartography". Comm. of the ACM, vol. 24, pp. 42-65, 1981.

[18] E.M. Mikhail, J.S. Bethel, J.C McGlone, "Introduction to Modern Photogrammetry", New York. John Wiley & Sons, Inc. 2001. 479 p.

[19] B.K. Horn "Closed-form solution of absolute orientation using unit quaternions," J. Opt. Soc. Am., vol. 4, pp. 629-642, 1987.